The Role of Conduction/Valence Bands and Redox Potential in Accelerated Mineral Dissolution

The dissolution kinetics of a number of manganese oxides in acidic solutions were studied. Using a slurry reactor, rate laws were determined for each of the manganese oxides in the hydrohalogen acids. Significant variations in the reaction rates (up to five orders of magnitude over the HCl base rate) were obtained with different acids. The addition of anions as neutral salts to acidic solutions is shown to produce the same rate-accelerating effect as acids containing that anion. The effect of the different acids on the oxide dissolution rates is explained using semiconductor band theory and energy diagrams.

S. E. LeBlanc, H. S. Fogler
Department of Chemical Engineering
University of Michigan
Ann Arbor, MI 48109

Introduction

The field of solid-liquid heterogeneous chemical reactions and catalysis is one that has not been studied extensively outside the field of electrochemistry. Dissolution reactions in particular have many widely varied applications, for example, in acid stimulation of oil reservoirs and in semiconductor etching. Another major application for dissolution reactions is to increase the production of existing strategic mineral resources that are vital to our national industries (Ember, 1981; Holden, 1981), and also to increase the number of economically feasible sources of these minerals. As a result there has been an increased emphasis on the development of improved extraction methods for ore treatments (Habashi, 1982; Ramirez and Gordon, 1982; Williams, 1978).

A major problem in these processes is the generally slow reaction rates. Therefore, acceleration of the dissolution rates of the desired metals and/or retardation of undesirable species to effect a separation would significantly enhance the recovery of valuable metals from mineral ores. While it is true that the dissolution rate of some minerals and mixed ore bodies is mass-transfer limited regardless of their particle size, a number of minerals (e.g., MnO_2, SnO_2, NiO) are reaction-rate limited at moderate particle sizes, and acceleration of these reaction rates would prove to be quite beneficial.

The acceleration or retardation of the dissolution rates of metals, oxides, and sulfides has been discussed in the electrochemical literature primarily with reference to corrosion. The effects of anions on the corrosion rates of metals are frequently conflicting. Jesionek and Szlarska-Smialowska (1983), for example, report the inhibition of the dissolution of iron in acidic solutions by halide ions, while Rostron (1979) and deCastro and Wilde (1979) report the breakdown of passivity (which amounts to accelerated dissolution) in the presence of halide ions.

The effect of anions on metal oxide dissolution has also been investigated. Majima et al. (1980) studied the dissolution of cupric oxide in acids using a rotating disk reactor and suggested that the adsorption of anions played an important role in the dissolution. No mechanism or rate laws were proposed for this effect. Awakura et al. (1980) provide an accurate assessment of the current state of the art in this research area: "Insufficient experimental data do not permit any definite conclusions."

Another important phenomenon is that some salts accelerate the rate of dissolution while others retard the rate. The work of Nii (1970) with NiO indicates that halide anions all depress the dissolution rate of NiO in sulfuric acid, with the iodide ion causing the largest rate depression. Garbouchian (1981), however, showed that the addition of iodide ions could dramatically accelerate the rate of dissolution of CuO in acidic solutions. Thus, in the case of the dissolution of CuO the iodide ion enhances the rate of dissolution greatly, while in the case of NiO it actually depresses the rate. This acceleration/retardation of the mineral reaction rates points out the possibility of new selective dissolution and separation techniques.

A number of mechanisms for oxide dissolution have been proposed in the literature. Warren and Devuyst (1973, 1975) and Grauer and Stumm (1982) have reviewed the leaching of metal oxides and proposed a general mechanism for the surface reactions consisting of surface hydroxylation, surface protonation,

Table 1. Manganese Oxide Mineral Data

Mineral	Crystal Structure	Mn Oxidation State	Mean Dia. μm	BET Surface Area m^2/g	Impurities ppm
MnO	Manganosite (FCC)	+2	100	0.445	Cobalt 50 Iron 100 Silicon 50
Mn_3O_4	Hausmannite (tetragonal)	+2, +3	5.5	3.120	Aluminum 50 Cobalt 50 Iron 100 Silicon 50
Mn_2O_3	Bixbyite (cubic)	+3	10.	0.709	Cobalt 50 Iron 250 Silicon 50
MnO_2	Pyrolusite (rutile)	+4	120	0.134	Iron 50 Silicon 50

(1976). They found that the redox potential of the solution had an effect on transition metal oxides, which are capable of forming oxides of variable stoichiometry. Reducing conditions increased the rate of dissolution of these oxides, while metals that form only one oxide (ZnO, MgO) were unaffected by the redox potential of the solvent. Detailed explanations for this phenomenon were not given. The present work elucidates the mechanism of this type of behavior for a family of manganese oxides.

Manganese oxide dissolution

Manganese oxides were chosen to investigate the phenomenon of enhanced mineral dissolution for several reasons:

1. They exhibit accelerated rates of dissolution in the presence of salts.

2. Manganese is an industrially important metal. It is a strategic mineral and is essential for steelmaking.

3. There has been increased interest in developing a hydrometallurgical treatment for seabed manganese nodules.

While there have been recent studies on the dissolution of manganese oxides by sulfur dioxide (Miller and Wan, 1983; Malati, 1983) and organic acids (Stone and Morgan, 1984a,b), the effect of anion addition or enhanced manganese oxide dissolution rates has not been thoroughly investigated. As will be shown, the selection of the anion in acidic solutions is an extremely important parameter when performing dissolution processes.

Experimental

Materials

Commercially available, powdered manganese oxides (Baker and Alfa) were used for these studies; their properties are sum-

and anion adsorption and desorption of a metal cation-anion complex. Other researchers (Vermilyea, 1966; Diggle, 1973) have attempted to explain the effects of anion and acid concentrations on the nonoxidative (or reductive) dissolution of ionic oxides in terms of ionic transfer across the double layer. Therefore, two general models have been popular in the oxide dissolution literature: adsorption-reaction-desorption, and electrochemical. Nicol (1983) analyzed these approaches and stated that the electrochemical aspects of the dissolution should be considered when formulating a dissolution model.

The effect of redox potential on the dissolution of several metal oxides (among these were oxides of Fe, Cu, Ni, and Mg) in hydrochloric acid was examined by Valverde and Wagner
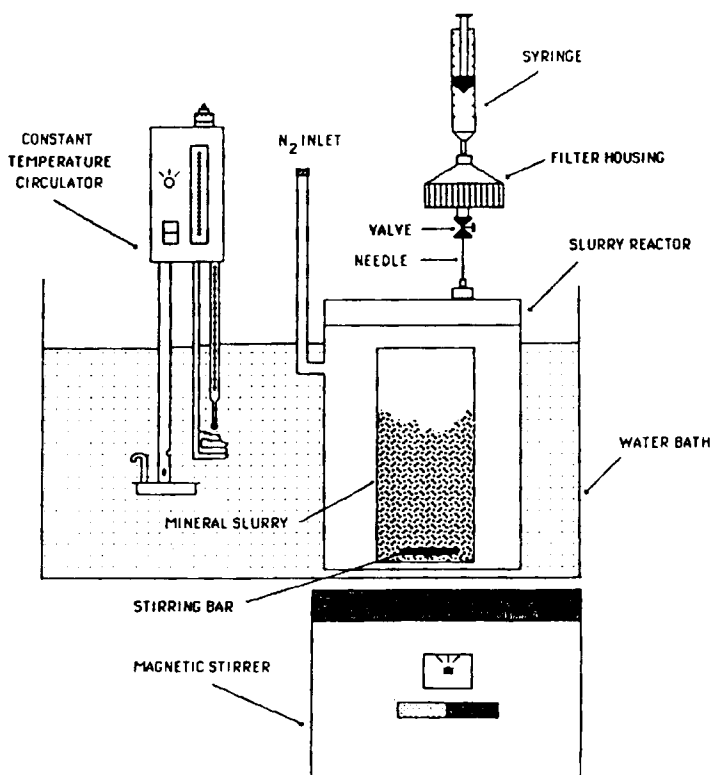

Figure 1. Slurry reactor apparatus.

marized in Table 1. Wide angle x-ray scattering (WAXS) was used to characterize the mineral structures. The specific surface areas were determined by the nitrogen adsorption (BET) method using a Quantasorb instrument. Arc emission spectroscopy and neutron activation analyses were performed on the pure oxides to determine the impurity levels indicated in the table. All other chemicals used were of reagent grade, and deionized water was used in the preparation of all the solutions.

Procedure

The dissolution reactions were conducted in 300–400 mL glass or polyethylene slurry reactors, shown in Figure 1. These were stirred sufficiently vigorously to completely suspend all the mineral particles. A water bath surrounding the reactor was used to maintain the temperature of the reaction volume at ±0.5°C. Samples of the dissolving slurry were rapidly withdrawn at short time intervals with a syringe and were filtered using 0.45 μm nitrocellulose filter membranes. Filtration of the mineral particles stopped the reaction in the sample aliquots so that they were representative of the product concentrations in solution as a function of time. The progress of the reaction was monitored by analyzing the sample aliquots for dissolved manganese with atomic absorption spectroscopy using a Perkin-Elmer model 503 AAS. Initial-rate experiments were conducted to investigate the dissolution kinetics of the manganese oxides. The initial-rate technique was used because the solid phase surface area and bulk phase solvent concentration are complex functions of the reaction time. Therefore, only at time $t = 0$ can the rates of dissolution be related accurately to the initial solvent concentration or measured surface area of the pure minerals. This technique for obtaining solid-liquid dissolution kinetics data has been demonstrated to provide reliable, reproducible information about the reaction rates (Kline and Fogler, 1981a–c).

Discussion of Results

The stable manganese species in solution is Mn^{+2} for the dissolution of manganese oxides in acidic solutions (Pourbaix, 1963). The overall dissolution reaction stoichiometry in the strong halogen acids for the manganese oxides under consideration here is shown in Table 2. The stoichiometry of these reactions was experimentally verified by performing a number of dissolution experiments with each manganese oxide.

The dissolution rate of MnO_2 in the halogen acids is shown in Figure 2. At 1.0 N acid concentration, the dissolution rate in HI is almost five orders of magnitude greater than the dissolution rate in HCl. Note also that the addition of iodide as NaI to HCl produces dissolution rate increases of the same order of magnitude as that of HI. This rate increase cannot be explained on the basis of different acid activities, as shown in Figure 3. From Figure 3 the activity coefficients of the acids vary by no more than

Table 2. Manganese Oxide Dissolution Stoichiometry in Strong Halogen Acids

$$MnO_2 + 4\,HX \rightarrow Mn^{+2} + 2X^- + 2H_2O + X_2$$

$$Mn_2O_3 + 6\,HX \rightarrow 2Mn^{+2} + 4X^- + 3H_2O + X_2$$

$$Mn_3O_4 + 8\,HX \rightarrow 3Mn^{+2} + 6X^- + 4H_2O + X_2$$

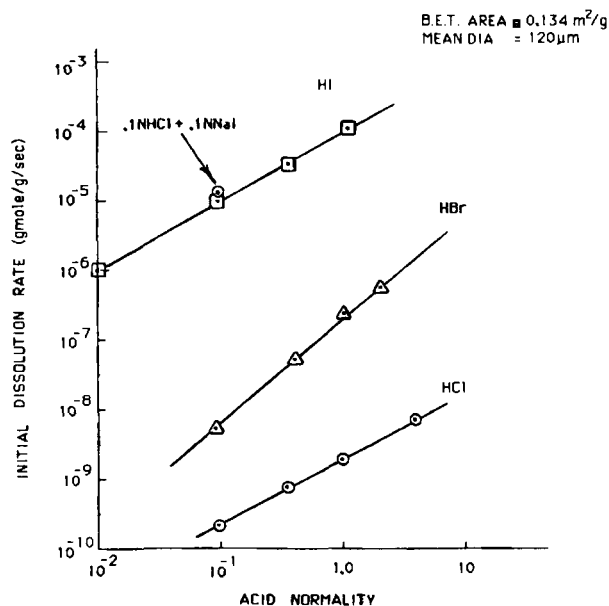$$MnO + 2HX \rightarrow Mn^{+2} + 2X^- + H_2O$$

Figure 2. Dissolution of MnO_2 in halogen acids at 25°C.

20% at 1.0 N acid concentration. This small difference in activity coefficients cannot conceivably explain such a large rate increase.

Similar plots of dissolution rate vs. acid normality are shown in Figures 4 through 6 for the other manganese oxides. The dissolution rates are always most rapid in HI and slowest in HCl. The rate law parameters and activation energies for the manganese oxides are listed in Table 3.

The low activation energies (18.8 kJ/gmol) for the dissolution of MnO in all the halogen acids, and the reaction orders near one indicate that these reactions are mass-transfer limited. The dissolution of MnO_2 in HI is mass-transfer limited as well ($n = 0.97$, $E_{act} = 18.4$ kJ/gmol). In addition, order of magnitude calculations were done to verify that the observed dissolution rates for these cases were indeed comparable to the expected mass transfer rates in solution. All other dissolution reactions shown in Table 3 fall in the surface reaction rate limited regime, as indicated by their relatively high activation energies ($E_{act} > 42$ kJ/gmol).

Since the dissolution of MnO is mass-transfer limited, we would expect that the initial dissolution rates in the halogen acids would be the same since the acid diffusion coefficients are nearly identical. Examination of Figure 6 indicates that the dissolution rate in HI > HBr > HCl. Scanning electron micro-

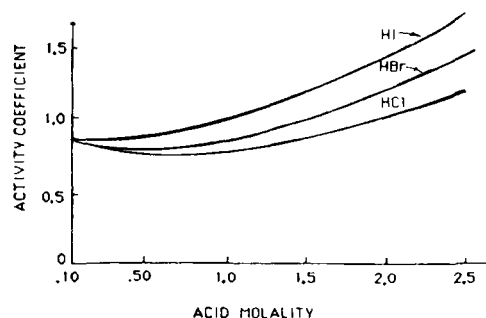Figure 3. Activity coefficients for halogen acids at 25°C.

B.E.T. AREA = 0.709 m²/g
MEAN DIA. = 10µm

Figure 4. Dissolution of Mn₂O₃ in halogen acids at 25°C.
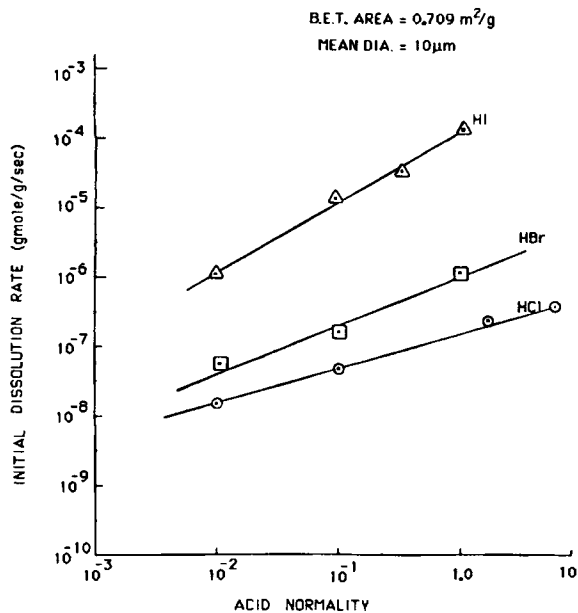
B.E.T AREA = 0.445 m²/g
MEAN DIA = 100µm

Figure 6. Dissolution of MnO in halogen acids at 25°C.

graphs (LeBlanc, 1985) of partially dissolved MnO in these acids reveals that the nature of the surface attack of MnO is different in these acids. The surface attack is uniform with HI, about 60% of the surface reacts initially with HBr, and only about 30% is initially attacked with HCl. These percentages were verified using SEM photographs of MnO particles at various stages of dissolution (LeBlanc, 1985). Since the dissolution of MnO is purely a chemical reaction (as opposed to electrochemical; i.e., no oxidation or reduction is required) the redox characteristics of the halogen anions cannot account for this difference. The heterogeneous nature of the mineral surface, however, provides a number of sites that are more susceptible to attack than others due to the presence of impurities, dislocations, crystal defects, etc. The iodide ion is much more polariza-
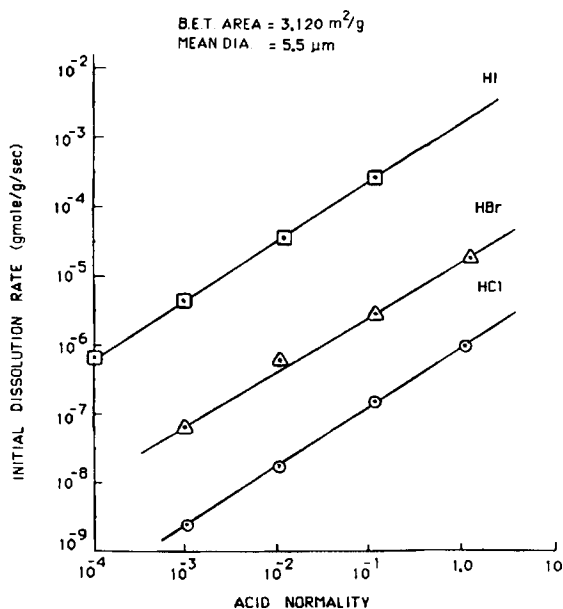
ble (i.e., its electron cloud is more easily deformed) and has a lower charge density than either bromide or chloride. This ability of the iodide ion to be easily polarized has been previously noted and is reponsible for stronger adsorption of iodide than bromide or chloride (Jesionek and Szlarska-Smialowska, 1983; Rostron, 1979; deCastro and Wilde, 1979). The difference in the degree of adsorption of the halides coupled with a distribution of surface energies on the MnO particles, arising from surface heterogeneities (Jansz, 1984) is responsible for the ordering of the rates shown in Figure 6.

The most interesting phenomenon to be explained regarding the dissolution of the manganese oxides is the dramatically larger rates produced by iodide ions than by chloride ions. This phenomenon is exhibited by MnO_2, Mn_2O_3, and Mn_3O_4. The manganese ions in these minerals must be reduced to the $+2$ oxidation state to be stable in solution (see Table 2). Table 1 shows the oxidation state of Mn in the oxides. Since the stable

B.E.T AREA = 3.120 m²/g
MEAN DIA = 5.5 µm

Figure 5. Dissolution of Mn₃O₄ in halogen acids at 25°C.

Table 3. Kinetic Parameter Summary for Mn Oxide Dissolution

Mineral	Acid	Reaction Order	Activation Energy E_{act} kJ/gmol
MnO	HI	0.87	18.0
	HBr	0.85	18.8
	HCl	0.83	20.1
Mn₃O₄	HI	0.93	56.5
	HBr	0.75	65.27
	HCl	0.87	84.1
Mn₂O₃	HI	0.85	47.7
	HBr	0.94	59.0
	HCl	0.59	96.7
MnO₂	HI	0.97	18.4
	HBr	1.4	42.3
	HCl	1.0	45.6

form of Mn in acidic solution is Mn, we might expect that the more reduced the Mn initially, the more easily the oxide will dissolve. The dissolution rates are summarized in Table 4. From this table, we can see that in general, the dissolution rates in each acid follows the trend of:

$$MnO > Mn_3O_4 > Mn_2O_3 > MnO_2 \qquad (1)$$
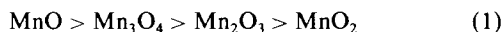
which supports the hypothesis that the more reduced the Mn in the mineral lattice, the more rapid the dissolution.

Effect of iodide ions on the dissolution

The dissolution rates of MnO_2, Mn_2O_3, and Mn_3O_4 in the halogen acids are ordered as follows:

$$HI > HBr > HCl \qquad (2)$$

To explain this phenomenon, one must examine the electrochemistry of the dissolution reactions.

Manganese oxides are semiconducting metal oxides (Samsonov, 1982). The electrochemistry of semiconductors has been discussed in relation to photoanodic dissolution and semiconductor electrode stability (Gerischer, 1978; Bard and Wrightson, 1977; Harris and Wilson, 1978), and these principles can be applied to freely dissolving semiconductor metal oxides, such as the manganese oxides, to explain the large disparity between the iodide, bromide, and chloride dissolution rates. The relationship between the energy levels in the semiconductor (valence band and conduction band) and the energy levels of oxidizing or reducing agents in the solution (i.e., their redox potential) is of critical importance.

We will consider the case of MnO for explanation of the iodide dissolution phenomenon (Mn_3O_4 and Mn_2O_3 are similar). MnO_2 is an intrinsic n-type semiconductor with a bandgap of 1.3 eV (Samsonov). In order for the manganese ions in the crystal to be reduced and mineral dissolution to occur, a reducing species in solution must donate electrons to the oxide crystal. The io-
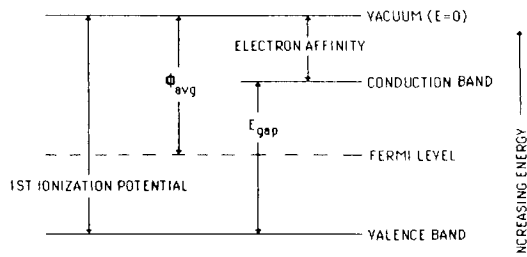
Table 4. Dissolution Rate Comparison of Mn Oxides in Halogen Acids

Acid	Temp.	MnO $K1$	Mn_3O_4 $K1$	Mn_2O_3 $K1$	MnO_2 $K1$
HI	0	1.46	259	84.8	14,200
	25	2.94	1,870	603	37,100
	40	3.98	6,340	1,280	46,900
	60			3,660	61,200
HBr	0	0.825	0.915	0.674	12.7
	25	1.5	9.75	5.54	75.8
	40	2.46	36.6	18.3	168
	60			72.3	346
HCl	0	0.494	0.044	—	—
	25	1.00	1.00	1.00	1.00
	40	1.56	4.98	6.43	2.92
	60	—	—	59.8	10.4
$K2$		18,800	26.7	12.7	1.00

$$K1 = \frac{\text{Rate constant}}{\text{Rate constant @25°C in HCl}}$$

$$K2 = \frac{\text{Rate constant in HCl @25°C}}{\text{Rate constant of } MnO_2 \text{ in HCl @25°C}}$$

Figure 7. Location of semiconductor band edges at point of zero charge (pzc).

dide, chloride, and bromide ions serve as the reducing species in the halogen acids being discussed. Gerischer has developed an energy model that allows one to predict whether electrons will be exchanged between a semiconductor and a electrolyte. The basis for the theory is to compare the energy levels of the valence band and the conduction band (the primary source and sink for electrons) of the semiconductor on the same energy scale as the redox couple of the solution. For MnO_2, whose bandgap is 1.3eV, it is necessary to locate the edges of the valence and conduction band to prepare such a diagram. The band edge position for a semiconductor can be estimated using the following equation (Morrison, 1980; Butler and Ginley, 1978), which is valid at the point of zero charge:

$$E^o_{\substack{conduction \\ band}} = -\frac{1}{2}(\phi_{Mn} + \phi_{O_2}) + \frac{1}{2}E_{gap} = -\phi_{avg} + \frac{1}{2}E_{gap} \quad (3)$$

where the ϕ term is the average work function of the constituent atoms (Morrison, 1980) and is a reflection of the energy level in the semiconductor at the Fermi level, relative to an electron in a vacuum. The Fermi level corresponds to the energy level in a semiconductor that has an equal probability of being occupied or unoccupied. For an undoped, intrinsic semiconductor, the Fermi level is located halfway between the lower edge of the conduction band and the upper edge of the valence band, Figure 7. The calculation locating the band edge for MnO_2 is shown below (Butler and Ginley; Morrison):

$$\phi_{Mn} = 4 \text{ eV} \qquad \phi_{O_2} = 7.28 \text{ eV}$$

$$E_{gap} = 1.3 \text{ eV}$$

$$E^o_{\substack{conduction \\ band}} = -\frac{1}{2}(4 + 7.28) + \frac{1}{2}(1.3) = -4.99 \text{ eV}$$

$$E^o_{\substack{valence \\ band}} = -\frac{1}{2}(4 + 7.28) - \frac{1}{2}(1.3) = -6.29 \text{ eV}$$

These values are estimates of the band edges at the point of zero

Table 5. Standard Reduction Potentials*

Reaction	V (SHE)**
$I_2 + 2e- \rightleftarrows 2I^-$	+0.536
$Fe^{+3} + e- \rightleftarrows Fe^{+2}$	+0.771
$Br_2 + 2e- \rightleftarrows 2Br^-$	+1.087
$Cl_2 + 2e- \rightleftarrows 2Cl^-$	+1.395
$Co^{+3} + e- \rightleftarrows Co^{+2}$	+1.840
$Mn_3O_4 + 8H^+ + 2e- \rightleftarrows 3Mn^{+2} + 4H_2O$	+1.824
$Mn_2O_3 + 6H^+ + 2e- \rightleftarrows 2Mn^{+2} + 3H_2O$	+1.443
$MnO_2 + 4H^+ + 2e- \rightleftarrows Mn^{+2} + 2H_2O$	+1.228

*From Pourbaix (1963) and Latimer (1952).
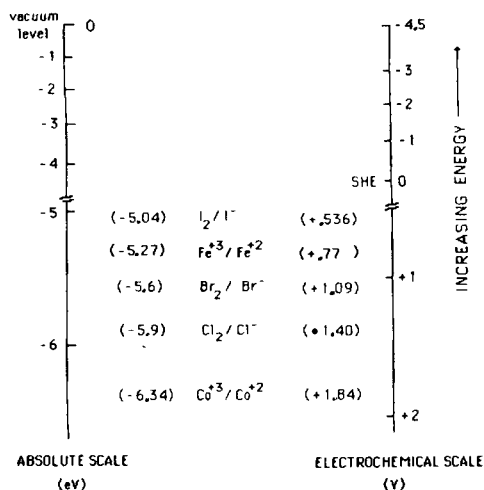**Standard hydrogen electrode.

Figure 8. Comparison of energy scales.

charge, or pH = 4.2 for MnO_2 (Leja, 1982). The band edges shift to lower energy levels by 59 meV/pH unit for a decreasing solution pH. Thus, since typical acid concentrations for the dissolution runs were 0.01 N to 1.0 N acid concentrations, we shall use pH = 1 as representative of typical pH values. Therefore the position of the band edges becomes:

Conduction band edge = −5.18 eV
Valence band edge = −6.48 eV

To compare the energy levels of the redox couples of species in solution (see Table 5 for relevant reduction potentials) with the semiconductor band edge energy levels, they must be placed on the same energy scale (Gerischer). The most common scale is the vacuum reference scale, i.e., the energy of an electron in a vacuum is chosen as the zero reference level. The energy level of the standard hydrogen electrode is −4.5 eV on this scale. Comparison of these two standard reference scales is shown in Figure 8 (Bard and Faulkner, 1980).

The difference between the energy levels of the solution redox couple and the semiconductor conduction band can be considered a potential barrier that the electrons must overcome for donation to the mineral lattice. This is shown schematically in Figure 9.

Figure 10 shows the relationship between the redox potentials for the halogen couples in solution and the energy bands in MnO_2. Electron transfer to the conduction band is clearly possible if the redox couple lies at a higher energy level than the conduction band, as is the case for the I_2/I^- couple. However the bromide and chloride couples lie within the band gap, which means electron donation by these anions will be more difficult. The existence of crystal defects, impurities, and broken bands at the lattice surface causes surface energy states to exist in the band gap of the material, as well as some band bending (Gerischer; Morrison). The bromide and chloride redox couples would be able to transfer electrons more easily to these surface states than to the conduction band and hence cause dissolution of the oxide as well. The barrier energies calculated from these
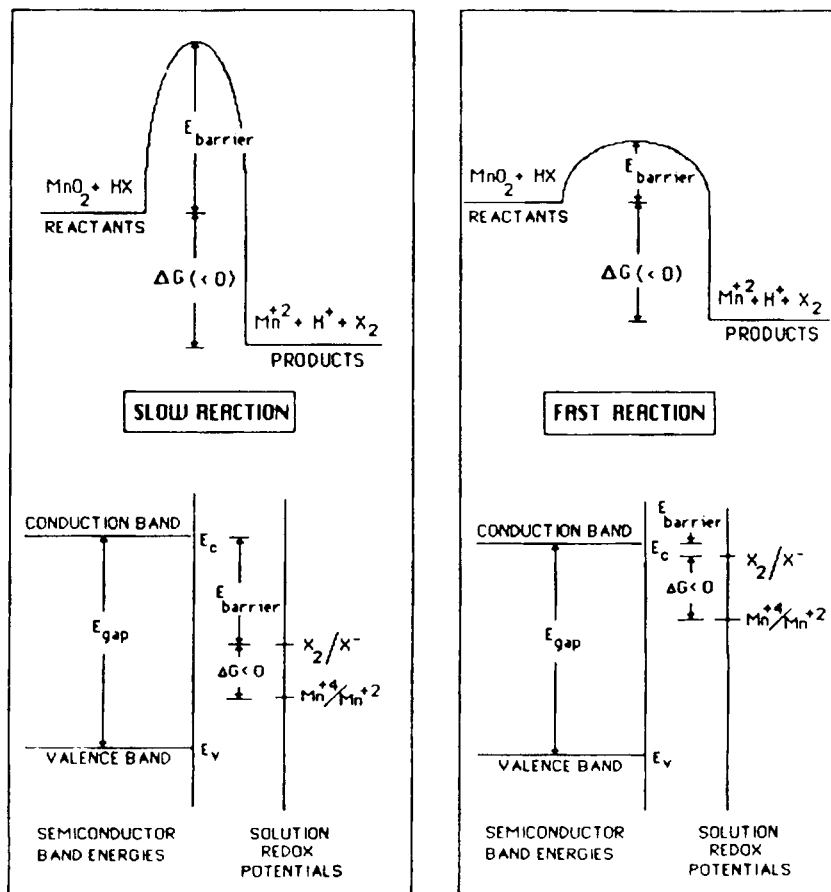

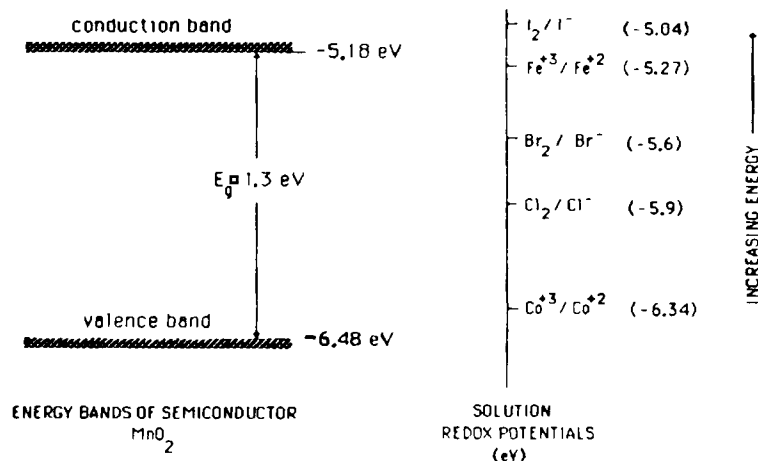Figure 9. Potential barriers for reductive oxide dissolution.

Figure 10. Relative energy levels for MnO₂ dissolution.

energy level differences (Cl⁻ = 69.5 kJ/gmol, Br⁻ = 40.5 kJ/mol) compare favorably with the experimentally determined activation energies, which further supports this mechanism.

In order to test this band theory, two other solution redox couples were chosen, Fe^{+2}/Fe^{+3} and Co^{+2}/Co^{+3}. The energy levels of these couples are shown in Figure 10. If the band theory is valid, then the iron couple should produce dissolution rates comparable to those of HI, since it lies very near the edge of the conduction band. On the other hand, the cobalt couple lies even lower than the chloride couple, so the dissolution rate should be very low. Figure 11 shows the dissolution rates of MnO₂ in the halogen acids as well as in acidic solutions containing the iron and cobalt couples. The iron couple does indeed accelerate the rate of dissolution of MnO₂ to virtually the identical level produced by HI, while cobalt has essentially no effect on the dissolution rate. The trends are as predicted by the model. The addition of iodide as NaI accelerates the rate of dissolution by HCl to virtually the same magnitude as that in HI. The same trends are observed for Mn₂O₃, as expected. The dissolution rate of MnO is unaffected by the presence of the iron and cobalt couples, due to the fact that no reduction of the Mn is necessary prior to mineral dissolution, and the reactions are already mass-transfer limited.
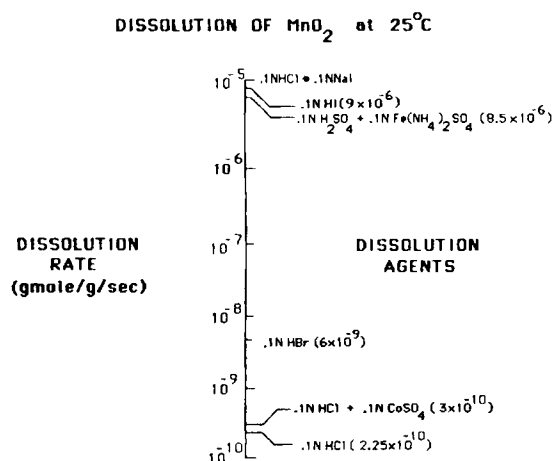

Figure 11. Effect of Fe and Co couples on MnO₂ dissolution.

The ability of the redox couple in solution to donate electrons to the mineral lattice is related to the difference between the energy band levels in the crystal and the redox potential of the couple in solution. The smaller this potential barrier for electron transfer, the higher the dissolution rates of the manganese oxides. This energy diagram model thus provides a convenient means for predicting the effectiveness of dissolution agents for hydrometallurgical processes as well as semiconductor etching.

Summary

The dissolution rates for the manganese oxides in acidic solution have been shown to be related to the oxidation state of the manganese in the lattice and the energy band levels in the oxide crystals. The more reduced the Mn is in the oxide, the more rapidly the oxide dissolves, for a given acid. The difference between the redox potential of the couples in solution and the conduction band energy level of the manganese oxides (for MnO₂, Mn₂O₃, and Mn₃O₄) was shown to be related to the rate of dissolution. This energy difference can be considered to be the potential barrier for electron transfer, which is required for reductive dissolution processes. Thus, the lower the barrier (i.e., the smaller the energy difference between the conduction band and the couple in solution), the more rapid the dissolution of the oxide. For MnO, which does not require reduction of the manganese prior to dissolution, the polarizability of the halide ions was related to the strength of the adsorption and the resultant difference in MnO dissolution rates. The more polarizable the anion, the more strongly it is adsorbed on the MnO surface, and the higher the dissolution rate.

The energy barrier concept relating the redox potentials of the couples in solution to the conduction/valence band energy levels provides a convenient means of predicting the effect of various ions in solution on reductive or oxidative dissolution processes. This procedure has applications in the field of hydrometallurgy as well as in semiconductor etching processes.

Literature cited

Awakura, Y., S. Kanei, and H. Majima, "Kinetic Study of the Nonoxidative Dissolution of Galena in Aqueous Acidic Solution," *Met. Trans. B.*, **11B**, 377 (1980).

Bard, A. J., and L. R. Faulkner, *Electrochemical Methods*, Wiley, New York (1980).

Bard, A. J., and M. S. Wrighton, "Thermodynamic Potential for the Anodic Dissolution of n-Type Semiconductors," *J. Electrochem. Soc.*, **124** (11), 1706 (1977).

Butler, M. A., and D. S. Ginley, "Prediction of the Flat Band Potentials at Semiconductor-Electrolyte Interfaces from Atomic Electronegativities," *J. Electrochem. Soc.*, **125** (2), 228 (1978).

DeCastro, M. A. C., and B. E. Wilde, "The Corrosion and Passivation of Iron in the Presence of Halide Ions in Aqueous Solution," *Corr. Sci.*, **19**, 923 (1979).

Diggle, J., ed., *Oxides and Oxide Films*, Dekker, New York, **2**, ch. 4 (1973).

Ember, L. R., "Many Forces Shaping Strategic Minerals Policy," *Chem. and Eng. News*, 20 (May 11, 1981).

Garbouchian, B. J., "Dissolution of Cupric Oxide in Acids," M.S. Thesis, Univ. Michigan (1981).

Gerischer, H., "Electrochemistry of the Excited Electronic State," *J. Electrochem. Soc.*, **125** (5), 218c (1978).

Grauer, R., and W. Stumm, "Die Koordinationschemie oxidischer Grenzflachen und irhe Auswirkung auf die Auflosungskinetik oxidischer Festphasen in wassrigen Losungen," *Colloid Polymer Sci.*, **260**, 959 (1982).

Habashi, F., "Hydrometallurgy," *Chem. and Eng. News*, 46, (Feb. 8, 1982).

Harris, L. A., and R. H. Wilson, "Semiconductors for Photoelectrolysis," *Ann. Rev. Mat. Sci.*, **8**, 99 (1978).

Holden, D., "Getting Serious about Strategic Minerals," *Science*, 305 (Apr. 17, 1981).

Jansz, J. J. C., "A Stochastic Modeling Approach to Chemically Controlled Dissolution of Ground Minerals," *Hydrometallurgy* **12**, 225 (1984).

Jesionek, M., and Z. Szlarska-Smialowska, "The Inhibition of the Dissolution of Iron in Sulfuric Acid by Halide Ions," *Corr. Sci.*, **23** (2), 183 (1983).

Kline, W. E., and H. S. Fogler, "Dissolution of Silicate Minerals by HF," *Ind. Eng. Chem. Fundam.*, **20**, 155 (1981a).

———, "Dissolution Kinetics—Catalysis by Strong Acids," *J. Coll. Interf. Sci.*, **82** (1), 93 (1981b).

———, "Dissolution Kinetics—Catalysis by Salts," *J. Coll. Interf. Sci.*, **82** (1), 93 (1981c).

Latimer, W. M., *The Oxidation States of the Elements and Their Potentials in Aqueous Solutions*, Prentice-Hall, Englewood Cliffs, NJ (1952).

LeBlanc, S. E., Ph.D. Thesis, "Enhanced Mineral Dissolution," Univ. Michigan (1985).

Leja, J., *Surface Chemistry of Froth Flotation*, Plenum, New York (1982).

Majima, H., Y. Awakura, T. Yazaki, and Y. Chikamori, "Acid Dissolution of Cupric Oxide," *Met. Trans. B.*, **11B**, 209 (1980).

Malati, M., in *Leaching and Diffusion in Rocks and Their Weathering Products*, S. S. Augustithis, ed., Theophrastus Pubs., Athens, p. 229 (1983).

Miller, J. D., and R. Y. Wan, "Reaction Kinetics for the Leaching Kinetics of Manganese Dioxide by Sulfur Dioxide," *Hydrometallurgy*, **10**, 219 (1983).

Morrison, S. R., *Electrochemistry of Semiconductor and Oxidized Metal Electrodes*, Plenum, New York (1980).

Nicol, M. J., in *Conf. Proc. Hydrometallurgy Research, Development and Plant Practice*, K. Osseo-Asare, and J. D. Miller (eds.), TMS-AIME, 177 (1983).

Nii, K., "On the Dissolution Behavior of NiO," *Corr. Sci.*, **10**, 571 (1970).

Pourbaix, M., *Atlas of Electrochemical Equilibria in Aqueous Solutions*, Pergamon (1963).

Ramirez, R., and H. Gordon, "New Resource from the Deep," *Chem. and Eng. News*, 37 (Feb. 8, 1982).

Rostron, A. J., "The Correlation Between Molecular Structure and the Tendency to Maintain or Destroy Iron Passivity in Aqueous Solution. Activation of Effectiveness of Anions Present Together with a Corrosion Inhibitor and/or an Oxidant," *Corr. Sci.*, **19**, 321 (1979).

Samsonov, G., *The Oxide Handbook*, 2nd ed., Plenum, New York (1982).

Stone, A. T., and J. J. Morgan, "Reduction and Dissolution of Manganese (III) and Manganese (IV) Oxides by Organics. 1: Reaction with Hydroquinone," *Env. Sci. Tech.*, **18** (6), 405 (1984a).

———, "Dissolution of Manganese (III) and Manganese (IV) Oxides in Organics. 2: Survey of the Reactivity of Organics," *Env. Sci. Tech.*, **18** (8), 617 (1984b).

Valverde N., and C. Wagner, "Considerations on the Kinetics and Mechanism of the Dissolution of Metal Oxides in Acidic Solution," *Ber. Bunsen-Gesellschaft*, **80**, 330 (1976).

Vermilyea, D. A., "The Dissolution of Ionic Compounds in Aqueous Media," *J. Electrochem. Soc.*, **113**, 1067 (1966).

Warren, I. H., and E. A. Devuyst, "Leaching of Metal Oxides," *Int. Sym. Hydrometallurgy*, D. J. Evans and R. S. Shoemaker, eds., AIME, Chicago (1973).

Warren, I. H., and E. A. Devuyst, *Int. Symp. Ser.*, "Fundamentals of the Leaching of Simple Oxides," *Hydrometallurgy*, 42, 7.1, London (1975).

Williams, N., "Studies of the Base Metal Deposits at McArthur River, Northern Territory, Australia. I: The Cooley and Ridge Deposits," *Econ. Geol. Bull., Soc. Econ. Geol.*, **73**, 1005 (1978).